Dynamic Registration of Cardiac US and CT Data Using Fourier Descriptors and Dynamic Time Warping

F. Tavard*†, A. Simon*†, A.I. Hernández*†, J. Betancur*†, E. Donal*†‡, M. Garreau*†
* INSERM, U1099, Rennes, F-35000, France;
† Université de Rennes 1, LTSI, Rennes, F-35000, France;
‡ CHU Rennes, Service de cardiologie et maladies vasculaires, Rennes, F-35000, France;

***Abstract*—Cardiac Resynchronization Therapy (CRT) can be optimized by the fusion of anatomical, functional and electrical information in a unified framework in order to identify the most effective pacing sites. The aim of this work is to perform a registration between dynamic CT and ultrasound (US) images (2D speckle tracking mode). The proposed registration approach is based on a contour to surface scheme, decomposed in four steps: (1) the temporal synchronization of data; (2) the segmentation of the left ventricle endocardial surface from the 3D+t CT data; (3) the segmentation and tracking of the myocardium from the 2D+t US data; (4) the registration of US contour with the CT surface. The originality of the method relies on the use of Fourier descriptors and Dynamic Time Warping (DTW) to handle different spatial and temporal resolutions as well as dissimilar cardiac rhythms between CT and US data. An evaluation on simulated data is described as well as results obtained on three patient databases.**

***Index Terms*—Multimodal registration, Dynamic Time Warping, Fourier descriptors, cardiac imaging, 3D dynamic CT, 2D US speckle tracking.**

I. Introduction

Nowadays, Cardiac Resynchronization Therapy (CRT) is accepted as a therapeutic option in heart failure patients who remain highly symptomatic despite optimized medical treatment. However, one third of the patients do not respond to the therapy [1]. Therefore, imaging modalities including echocardiography or magnetic resonance imaging, aimed at mechanical dyssynchrony estimation, have been proposed to improve patient selection criteria and lead placement [1], [2]. The most challenging task to carry out remains both the identification of the most effective pacing sites and the guidance of the left ventricular lead implantation using a venous access.

Our goal is to better plan the placement of CRT leads using anatomical, functional and electrical data acquired with cardiac Computed Tomography (CT) imaging, ultrasound (US) imaging and electro-anatomical maps (EAM) respectively. Previous works have demonstrated the abilities of CT to analyse both venous structures and left ventricle function [3], [4]. First approaches have been proposed to solve registration problems between CT and EAM data [5] and between CT and US data [6].

This paper focuses on the registration of 3D dynamic cardiac CT data and 2D dynamic echocardiographic images (2D speckle tracking mode) in order to match a high resolution anatomical description of both the LV and the veins with functional information (displacement or strain). This task is not straightforward mainly because CT and US data are acquired in different conditions of spatial dimension (3D vs. 2D) and of spatial and temporal resolutions (50 ms vs. 15 ms for temporal sampling). The nature of the observed information is also different: CT imaging provides high resolution information of the endocardial and epicardial surfaces whereas US speckle imaging provides the extraction of a contour describing the myocardium. Moreover the two medical exams are not realized simultaneously (one or two days between the two acquisitions), implying uncertainties on the similarity of the cardiac rhythms.

Very few works have been proposed in the literature for multimodal cardiac data registration considering 2D US data [7] or 3D US data in spite of recent advances [8]. The goal of these works is mainly to compare pre- and per-operative data during surgical gestures guided by US [9], or to combine complementary descriptors to help in diagnosis [10]. The temporal synchronization of data is often the first problem to solve. Some works use the ECG by considering only one instant related to the same cardiac phase [11], whereas others use a dynamic registration relying on an interpolation process [10], [12]. The proposed approaches can be classified in: (1) stereotactic methods that need the identification of the US probe position in pre-operative data (registered with MRI data), and in real time during the operation [9], [10], [13]; (2) iconic methods based on mutual information that has been applied to 2D US images [12] but also to 3D and IVUS images [13]; (3) geometrical methods that need the definition of geometrical landmarks given during the acquisition in MRI/US registration [14] or by user interaction in PET/US registration [15]; (4) modeling methods that are based on the simulation of US images from CT data allowing, for example, the disposal of the temporal synchronization step [10]. All these methods show encouraging results, however they are highly dependent on pre-processing steps and manual interaction.

The proposed dynamic registration approach is based on a contour to surface registration scheme, the contour being

978-1-4673-2584-4/12/$31.00 ©2012 IEEE

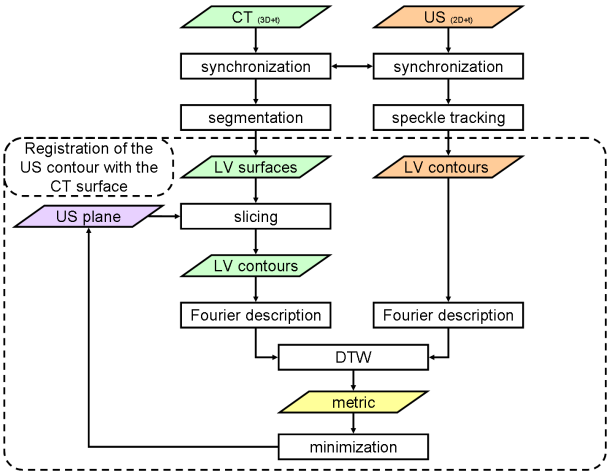

Fig. 1. Framework of the proposed approach.

extracted from US data and the left ventricle endocardial surface from CT data. The originality of this method first comes from the combination of Fourier descriptors to handle different spatial resolutions between 3D and 2D processed data with Dynamic Time Warping (DTW) to handle different cardiac rhythms and time samplings between CT and US data. The paper is organized as follows: the registration method is described step-by-step, then an evaluation on simulated data is given, finally first results obtained on three patient databases are presented, discussed in a qualitative way, and followed by our conclusions.

II. Method

The proposed approach is depicted by Fig. 1. It is composed of four main phases:

- synchronization of CT and US data according to the peak of the QRS complex
- segmentation of the endocardial surface from the 3D+t CT data ; a dynamic surface is obtained
- segmentation and tracking of the myocardium from the 2D+t US data ; a dynamic contour is obtained
- registration of US dynamic contour with the CT dynamic surface.

These four phases are described in the following sections, focusing on the registration method which is the main goal of this work.

A. Synchronization on the QRS complex peak

Both original data (CT and US) are dynamic. In order to synchronize them, the peak of the QRS complex is considered in both modalities. Considering US, this peak is simply extracted from the ECG acquired during the exam. Considering the CT acquisition, the ECG is not recorded but the acquisition is synchronized according to the peak of the QRS complex. Therefore, the first time-instant corresponds to this peak.

B. CT Data Segmentation

CT imaging is useful for the 3D visualization of coronary vessels (arteries and veins). Combining multi-detector and gantry high rotation speed, Multi-Slice CT (MSCT) allows dynamic cardiac acquisition with a high spatial resolution. In order to segment the left endocardium over the cardiac cycle, we use a segmentation method based on a fuzzy connectedness algorithm [16], the results have been visually validated by a medical expert. The segmented surfaces are then reconstructed. The left ventricle is automatically separated from the left auricle using an estimation of the position of the mitral plane [6]. Next the coordinates of the apex and of the great axis are estimated.

C. US Data Segmentation and 2D speckle tracking

Speckle tracking is an image processing method that is extensively used to assess cardiac motion from 2D dynamic echocardiographic images [17]. Routine B-mode images are analyzed for frame-by-frame movement of stable patterns of natural acoustic markers, or speckles, present in US images over the cardiac cycle. The tracking relies on the manual selection of the endocardial contour. It is then extended to consider the whole myocardium and decomposed in segments (about 60 in long-axis view, 40 in short-axis view). Speckle tracking enables to track these segments and therefore to provide a dynamic representation of the cardiac contour.

D. Registration of the 2D+t US contour and the 3D+t CT surface

The registration method relies on the search of the US acquisition plane in the 3D CT volume. For this purpose, the proposed metric is based on the dynamic matching of the 2D+t cardiac contour extracted from US images with the 3D+t endocardial surface segmented from the CT images. The search of the US acquisition plane is performed by optimizing the position of a plane used to slice through the segmented 3D surface. For each tested position of the plane, a metric is computed between the two 2D+t contours. The computation of this metric relies on:

(i) Fourier descriptors: spatial resolution in US and CT data differs significantly. To match contours with the same level of details, Fourier descriptors are used to describe the shapes.

(ii) Dynamic time warping (DTW) and dynamic programming: in order to handle variations of the cardiac cycle dynamic between both acquisitions, dynamic time warping is applied in the Fourier descriptors space.

Each step is described in the following sub-sections.

1) Optimization of the US acquisition plane positioning: The position of the US contour in the CT coordinate system is given by seven parameters (Fig. 2): $\overrightarrow{O} = (x_o, y_o, z_o)$ the origin of the acquisition plane P_{US}, $\overrightarrow{N_{US}} = (x_N, y_N, z_N)$ the normal of P_{US} and θ_N the rotation angle around $\overrightarrow{N_{US}}$.

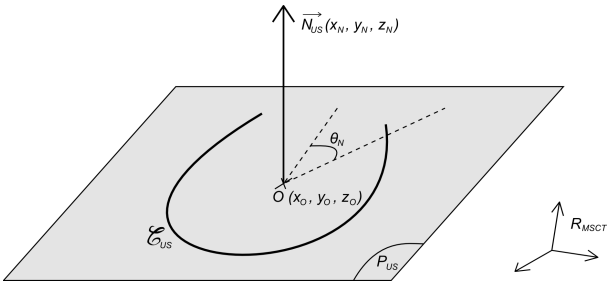

Fig. 2. Parameters defining the position of a US contour in the CT referential.

Once a position of the plane is defined, the plane is used to slice through the dynamic CT surface resulting in one dynamic contour. A metric, based on Fourier descriptors and dynamic time warping (eq. 5) is then used to evaluate the quality of the match between both contours. This metric is used to optimize the seven parameters defining the position of P_{US}, using a gradient descent. The optimization is initialized assuming the following: the apex is considered as the origin O and $\overrightarrow{N_{US}}$ is chosen as the vector forming a 90° angle (for the 4-chambers view) or 180° (for the 2-chambers view) with $\overrightarrow{GA} \wedge \overrightarrow{Z}$ ($\overrightarrow{GA}$ being the great axis of the LV and $\overrightarrow{Z}$ the CT coordinate axis).

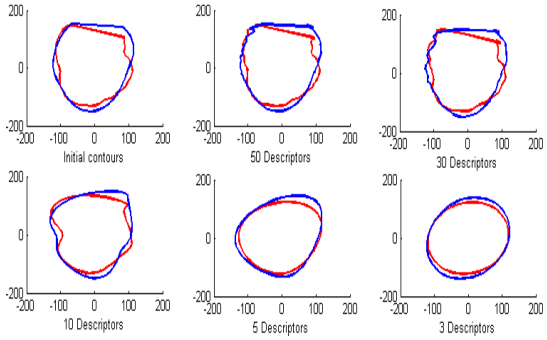

Fig. 3. CT (red) and US (blue) contours as a function of Fourier descriptors' order (upper left: original contours).

2) Contours decomposition by Fourier descriptors: Let $\mathscr{C}$ be a contour composed of N ordered (e.g. clockwise) points labelled z_n, $n \in \{0, \ldots, N-1\}$ in the complex space ($z_n = x_n + i.y_n$). The Fourier descriptors Z_k are obtained by using the discrete Fourier transform:

$$Z_k = \sum_{n=0}^{N-1} z_n \exp(-\frac{2i\pi}{N}.kn) \tag{1}$$

These descriptors are translation- (by setting $Z_0 = 0$) and rotation- (when considering only the coefficients' modulus) invariant. The maximum considered order has been selected as $K = 50$ because it provides a precise enough description (Fig. 3). Moreover, in order to give more importance to the first components, a weight inversely proportional to the order was applied. Finally, we have:

$$Z'_k = \frac{1}{k+1}\|Z_k\| \tag{2}$$

which is defined for both modalities and for each of their time-instant : $Z'_{CT_k}(t_{CT})$ and $Z'_{US_k}(t_{US})$ with $k = 1, \ldots, K$; $t_{CT} = 1, \ldots, T_{CT}$ and $t_{US} = 1, \ldots, T_{US}$ (T_X being the number of frames acquired by the modality X).

3) Dynamic Time Warping based metric: Dynamic Time Warping (DTW) [18] enables to measure similarity between two sequences which may vary in time or speed. The sequences are then warped non-linearly in the time dimension. For this purpose, DTW is based on the search for a warping function $F = \{(i_1, j_1), (i_2, j_2), \ldots, (i_N, j_N)\}$ which is a sequence of N couples of (t_{CT}, t_{US}) such that a distance $D(F)$ is minimized. This distance is defined to optimize the match between the Fourier descriptors along the cardiac cycle: $D(F) = \sum_{n=1}^{N} d(i_n, j_n).w(i_n, j_n)$, where $d(i_n, j_n)$ is the distance between the two contours at times i_n and j_n : $d(i_n, j_n) = [\sum_{k=0}^{k=50}(Z'_{CT_k}(i_n) - Z'_{US_k}(j_n))^2]^{1/2}$, and $w(i_n, j_n)$ is a weight (with a classical symmetric form) introduced to compensate the variation of the path length:

$$w(i_n, j_n) = (i_n - i_{n-1} + (j_n - j_{n-1})) \tag{3}$$

Some classical restrictions on the warping function are added in order to preserve the structures of both cardiac cycles:

(i) Monotonic conditions: $i_n \geq i_{n-1}$ and $j_n \geq j_{n-1}$

(ii) Continuity conditions: $i_n - i_{n-1} \leq 1$ and $j_n - j_{n-1} \leq 1$

(iii) Boundary conditions: $i_1 = 1$, $i_N = T_{CT}$, $j_1 = 1$ and $j_N = T_{CT}$

(iv) Slope constraint condition: to avoid unrealistic correspondences, the gradient of F should not be too steep or too gentle. If a couple (i, j) moves forward in the horizontal or vertical direction, it is not allowed to step further in the same direction before stepping once in the diagonal direction.

4) Dynamic programming: In order to find the warping function F minimizing $D(F)$ and following the previous constraints, dynamic programming is used. The minimization is seen as the computation of a sequence g_k using the following recursive algorithm:

(i) Initial condition: $g(i_1, j_1) = 2d(i_1, j_1)$

(ii) Dynamic programming equation:

$$g(i,j) = \min \begin{bmatrix} g(i-1, j-2) + 2d(i, j-1) + d(i,j), \\ g(i-1, j-1) + 2d(i,j), \\ g(i-2, j-1) + 2d(i-1, j) + d(i,j) \end{bmatrix} \tag{4}$$

(iii) Time-normalized distance of the optimized warping function F_{opt} :

$$D(F_{opt}) = \frac{1}{T_{CT} + T_{US}} g(T_{CT}, T_{US}) \tag{5}$$

Moreover, the search domain has been restricted using a combination of Itakura's parallelogram ([19]) and Sakoe's ribbon ([18]) (Fig. 4).

III. Evaluation on simulated data

An evaluation of the proposed metric is carried out on simulated data.

A. Data simulation

Dynamic US contours are simulated in order to evaluate the proposed metric. Four steps compose the process used to obtain the simulated contours:

(i) the acquisition plane is defined arbitrarily and used to cut through the 3D+t CT surface, generating 2D+t contours;

(ii) the position in space of the points defining the contours is smoothed using a sinc kernel filtering;

(iii) the 2D+t contours were interpolated over time to get as many instants in the simulated data as there is in a standard US acquisition (about 70 instants in the cardiac cycle);

(iv) finally, the 2D+t contours are scaled to match the size of a myocardial contour rather than endocardial. The scale factor is 110%.

Elementary transforms were applied to the simulated 2D+t contours. Three parameters have been tested : the translation along the US plane's normal, the rotation around an orthogonal axis to the same normal, and the rotation around the great axis (Fig. 5).

The metric value (eq. 5) is then computed between the 3D+t CT surfaces and the transformed simulated 2D+t contours. Figure 6 provides a comparison between the proposed metric and the sum of squared Euclidean distances between the contours at the first instant.

B. Metric values

The metric evolution in the translation and rotations described, is given Fig. 6. The minimum of the metric in each case is pointed by an arrow. For the two first elementary transforms (translation along the US plane's normal and rotation around an orthogonal axis to the same normal), the minimum value of the metric is reached for the initial position of the simulated contours. Considering the rotation around the great axis, the minimum value is reached for a rotation of 5° around the great axis (i.e. an error of 2.7%).

Moreover, this metric shows two maxima around $-100°$ and $100°$ (in the case of the rotation around the great axis). Those rotations represent conditions for which contours are distant (in terms of the metric). As the shape of the left ventricle endocardium is almost a surface of revolution, the two maxima point out the fact that not only the geometric but mainly the dynamic component is predominant in the proposed metric.

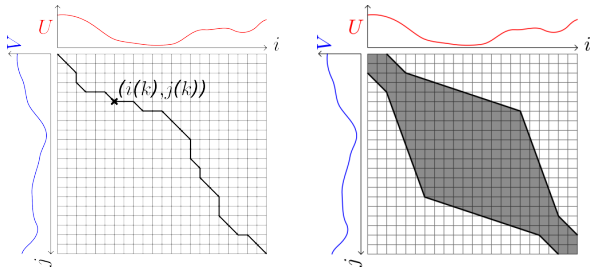

Fig. 4. Left: dynamic time warping between two signals U and V. Right: restriction domain on the search space.

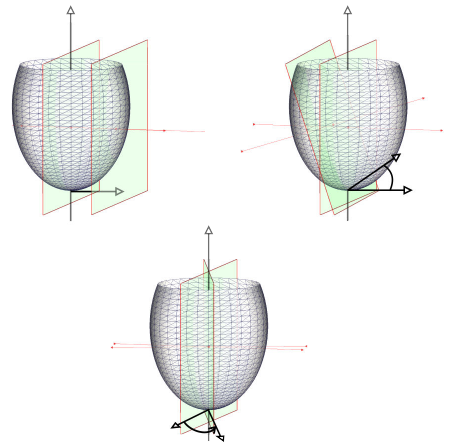

Fig. 5. Illustration of the three tested parameters for the metric evaluation. Top left: translation along the US plane's normal. Top Right: rotation around an orthogonal axis to the same normal. Bottom: rotation around the great axis.

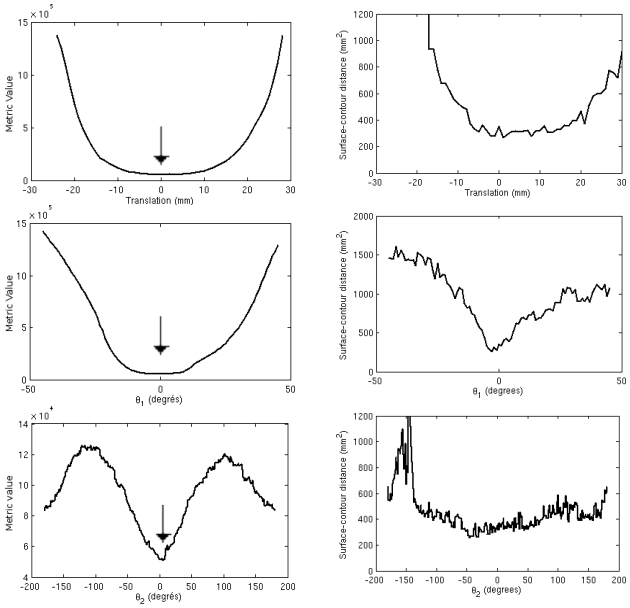

Fig. 6. Metric as a function of the three elementary transforms applied to the simulated 2D+t contours (left) compared to the distance (sum of squared distance) between first instants contour and surface (right). Top: translation along the US plane's normal. Middle: rotation around an orthogonal axis to the same normal. Bottom: rotation around the great axis. The arrows point at the minimum for each case.

The visualization of the metric in a neighbourhood of a minimum position shows few local minima and a global minima rather well defined. Those specificities of the metric allow the use of a gradient descent optimization. Also, the comparison with a more classical metric (sum of squared Euclidean distances) - which presents many local minima - proves the efficiency of the proposed metric.

IV. Results

The proposed method has been applied on the data of three different patients, candidates for CRT. For one patient, only the 4-chambers view was available and the result of the proposed

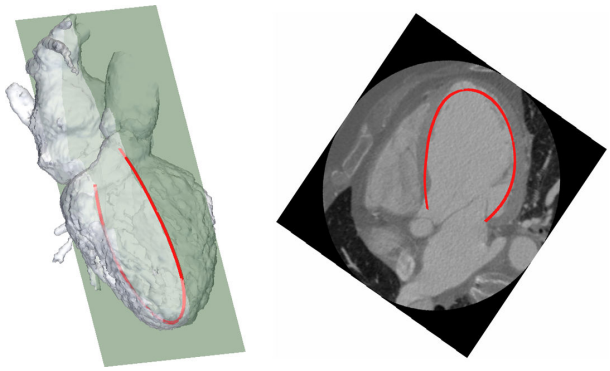

Fig. 7. Left: segmented surface from the CT data and US plane result after registration. Right: superposition of the US contour and the corresponding CT slice (4-chambers view).

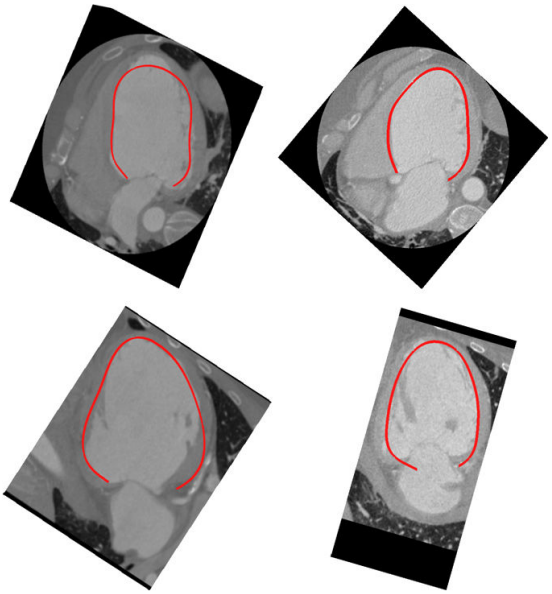

Fig. 8. Superposition of the US contour and the corresponding CT slice (Left/right columnns: two different patients; Upper (resp. lower) row: 4- (resp. 2-) chambers view).

approach is represented at Fig. 7. For the two other patients, the US acquisition included both 2- and 4-chambers views. The superposition of the US contour and the corresponding CT slice is presented at Fig. 8.

The qualitative assessment of all results is satisfactory. All the obtained US acquisition planes are realistic, as for the relative positions of the two views when available. The major differences between the US contour and the CT data are localized in the apical segments which can be explained by a well-known problem: the difficulty to visualize the apical area in echography.

These results have been presented to an echocardiographic expert who has evaluated them as being reliable.

V. Conclusion and perspectives

In this work, we propose a method to register 2D+t US acquisitions with 3D+t CT data. To deal with the important differences of these two modalities in terms of spatial resolution, we used Fourier descriptors to describe the contours extracted from US and CT data. In order to handle the dissimilarity in the cardiac rhythms, dynamic time warping was used on the geometrical description of the heart to estimate the temporal match between the two descriptions. The proposed metric has been evaluated on simulated data, giving an error of 2.7%. The results obtained on three patients have been evaluated by a medical expert as being reliable. Future works will deal with the estimation of descriptors based on the fusion of the functional information provided by echography with the anatomical information provided by CT and with electrical information given by electro-anatomical mapping. Moreover, in a time where 3D+t US is the new trend in cardiac echography, the proposed metric could be easily transcribed to surfaces rather than contours.

References

[1] J.M. Morgan and V. Delgado, "Lead positioning for cardiac resynchronization therapy: techniques and priorities," *Europace*, vol. 11, no. suppl 5, pp. v22–v28, 2009.

[2] E.S. Chung, A.R. Leon, L. Tavazzi, J.P. Sun, P. Nihoyannopoulos, J. Merlino, W.T. Abraham, S. Ghio, C. Leclercq, J.J. Bax, et al., "Results of the predictors of response to CRT (PROSPECT) trial," *Circulation*, vol. 117, no. 20, pp. 2608–2616, 2008.

[3] J. Coatrieux, A. Hernandez, P. Mabo, M. Garreau, and P. Haigron, "Transvenous path finding in cardiac resynchronization therapy," *Functional Imaging and Modeling of the Heart*, vol. 45, pp. 876–878, 2005.

[4] M. Garreau, A. Simon, D. Boulmier, J.L. Coatrieux, HL Breton, et al., "Assessment of left ventricular function in cardiac MSCT imaging by a 4D hierarchical surface-volume matching process," *International Journal of Biomedical Imaging*, vol. 2006, pp. 10, 37607.

[5] F. Tavard, A. Simon, C. Leclercq, D. Pavin, A. Hernandez, and M. Garreau, "Data fusion of left ventricle electro-anatomical mapping and multislice computerized tomography," in *Image Processing (ICIP), 2009 16th IEEE International Conference on*, nov. 2009, pp. 1745 –1748.

[6] F. Tavard, A. Simon, E. Donal, AI Hernández, and M. Garreau, "Fusion of MSCT imaging, electro-anatomical mapping and speckle tracking echocardiography for the characterization of local electro-mechanical delays in CRT optimization," in *Computers in Cardiology, 2010*. IEEE, 2010, pp. 401–404.

[7] T. Mäkelä, P. Clarysse, O. Sipila, N. Pauna, Q.C. Pham, T. Katila, and I.E. Magnin, "A review of cardiac image registration methods," *Medical Imaging, IEEE Transactions on*, vol. 21, no. 9, pp. 1011–1021, 2002.

[8] F. Li, P. Lang, M. Rajchl, E.C.S. Chen, G. Guiraudon, and T.M. Peters, "Towards real-time 3d us-ct registration on the beating heart for guidance of minimally invasive cardiac interventions," in *Proceedings of SPIE*, 2012, vol. 8316, p. 831615.

[9] Q. Zhang, R. Eagleson, and T.M. Peters, "Real-time visualization of 4D cardiac MR images using graphics processing units," in *Biomedical Imaging: Nano to Macro, 2006. 3rd IEEE International Symposium on*. IEEE, 2006, pp. 343–346.

[10] W. Wein, A. Khamene, D.A. Clevert, O. Kutter, and N. Navab, "Simulation and fully automatic multimodal registration of medical ultrasound," *Medical Image Computing and Computer-Assisted Intervention–MICCAI 2007*, pp. 136–143, 2007.

[11] M.J. Ledesma-Carbayo, J. Kybic, M. Desco, A. Santos, M. Suhling, P. Hunziker, and M. Unser, "Spatio-temporal nonrigid registration for ultrasound cardiac motion estimation," *Medical Imaging, IEEE Transactions on*, vol. 24, no. 9, pp. 1113–1126, 2005.

[12] X. Huang, N. Hill, J. Ren, G. Guiraudon, and T. Peters, "Intra-cardiac 2D US to 3D CT image registration," in *Proceedings of the SPIE International Symposium on Medical Imaging. San Diego, CA*, 2007.

[13] X. Huang, J. Moore, G. Guiraudon, D.L. Jones, D. Bainbridge, J. Ren, and T.M. Peters, "Dynamic 2D ultrasound and 3D CT image registration of the beating heart," *Medical Imaging, IEEE Transactions on*, vol. 28, no. 8, pp. 1179–1189, 2009.

[14] J. Hong, K. Konishi, H. Nakashima, S. Ieiri, K. Tanoue, M. Nakamuta, and M. Hashizume, "Integration of MRI and ultrasound in surgical navigation for robotic surgery," in *World Congress on Medical Physics and Biomedical Engineering 2006*. Springer, 2007, pp. 3052–3055.

[15] A. Savi, M.C. Gilardi, G. Rizzo, M. Pepi, C. Landoni, C. Rossetti, G. Lucignani, A. Bartorelli, and F. Fazio, "Spatial registration of echocardiographic and positron emission tomographic heart studies," *European Journal of Nuclear Medicine and Molecular Imaging*, vol. 22, no. 3, pp. 243–247, 1995.

[16] J. Fleureau, M. Garreau, A. Simon, R. Hachemani, and D. Boulmier, "Assessment of global cardiac function in msct imaging using fuzzy connectedness segmentation," in *Computers in Cardiology, 2008*. IEEE, 2008, pp. 725–728.

[17] S. Langeland, J. Dâhooge, H. Torp, B. Bijnens, and P. Suetens, "Comparison of time-domain displacement estimators for two-dimensional RF tracking," *Ultrasound in medicine & biology*, vol. 29, no. 8, pp. 1177–1186, 2003.

[18] H. Sakoe and S. Chiba, "Dynamic programming algorithm optimization for spoken word recognition," *Acoustics, Speech and Signal Processing, IEEE Transactions on*, vol. 26, no. 1, pp. 43–49, 1978.

[19] F. Itakura, "Minimum prediction residual principle applied to speech recognition," *Acoustics, Speech and Signal Processing, IEEE Transactions on*, vol. 23, no. 1, pp. 67–72, 1975.